Q_y-Excitation Resonance Raman Scattering from the Special Pair in *Rhodobacter sphaeroides* Reaction Centers. Implications for Primary Charge Separation†

Vaithianathan Palaniappan,‡ Mila A. Aldema,§ Harry A. Frank,§ and David F. Bocian*,‡

Department of Chemistry, University of California, Riverside, California 92521, and Department of Chemistry, University of Connecticut, Storrs, Connecticut 06269

Received May 5, 1992; Revised Manuscript Received August 5, 1992

ABSTRACT: Q_y-excitation resonance Raman (RR) spectra are reported for reaction centers (RCs) from *Rhodobacter sphaeroides* 2.4.1. The RR spectra were acquired for both chemically reduced and oxidized RCs at 25 and 201 K by using a variety of excitation wavelengths in the range 800–920 nm. This range spans the Q_y absorption bands of the special pair (P) and the accessory bacteriochlorophylls (BChls). The RR studies indicate that both P and the accessory BChls exhibit rich RR spectra in the 30–1800-cm^{-1} region. For both types of pigments, at least 20 bands are observed in the 30–750-cm^{-1} range. Although the frequencies of the modes of P and the accessory BChls are different, it is possible to make one-to-one correlations of the bands observed for the two types of pigments. This result suggests that the vibronically active low-frequency modes of P are derived from monomer-like vibrations (although they may be coupled monomer-like modes) rather than being vibrations resulting from the additional degrees of freedom present in the dimer. A plausible set of vibrational assignments for the low-frequency modes of both P and the accessory BChls is proposed on the basis of a semiempirical normal coordinate calculation. Comparison of the RR intensities of the low-frequency modes of P with those of the analogous modes of the accessory BChls indicates that the intensities of the modes of the former pigments are considerably larger than those of the latter. Collectively, the spectral data indicate that a large number of low-frequency modes of P are strongly coupled to the Q_y electronic transition. Simulations of the absorption spectrum indicate that the average electron–phonon coupling parameter $S \sim 0.3$ for modes below 200 cm^{-1} and $S < 0.05$ for modes in the 200–750-cm^{-1} region. The former group of modes are predominantly out-of-plane deformations whereas the latter exhibit some out-of-plane character. It is suggested that the unusually large electron–phonon coupling for the out-of-plane modes arises because these deformations modulate the charge-transfer character of the Q_y-excited state of P.

The primary charge separation event in bacterial photosynthesis occurs in a membrane-bound protein designated as the reaction center (RC)[1] (Budil et al., 1987; Kirmaier & Holten, 1987; Deisenhofer & Michel, 1989a; Feher, 1989; Friesner & Won, 1989; Boxer et al., 1989). The X-ray crystal structures reported for RCs provide the starting point for establishing a detailed description of the factors that mediate light-induced electron transfer (Deisenhofer et al., 1985; Chang et al., 1986; Allen et al., 1986; Deisenhofer & Michel, 1989b). The donor state in the initial charge-separation process is the lowest-lying singlet excited state (P*) of a pair of electronically coupled bacteriochlorophyll (BChl) molecules (Kirmaier & Holten, 1987; Boxer et al., 1989; Friesner & Won, 1989). The absorption band for this state is quite broad and occurs at unusually low energy (10 000–12 000 cm^{-1}) (Holten & Kirmaier, 1988) and exhibits distinctive hole-burned (Meech et al., 1985, 1986; Boxer et al., 1986a,b; Hayes & Small, 1986; Hayes et al., 1988; Tang et al., 1988; Johnson et al., 1989, 1990) and Stark effect (Lösche et al., 1987, 1988; Lockhart & Boxer, 1987, 1988) spectra. These properties of P* have been analyzed in attempts to explain both the directionally and mechanism of electron transfer (Warshel et al., 1988; Plato et al., 1988; Won & Friesner, 1988a,b; Friesner & Won, 1989; Boxer et al., 1989).

Most studies of P* have used optical spectroscopic techniques. Recently, the P* state has also been probed via resonance Raman (RR) spectroscopy (Donohoe et al., 1990; Shreve et al., 1991). RR studies are particularly appealing because the vibrational spectra are well resolved and the modes that gain enhancement are those that exhibit the largest vibronic activity (Myers & Mathies, 1987). Knowledge of the frequencies and Franck–Condon factors of the vibronically active modes is required for construction of detailed models of the charge-separation process. Unfortunately, Q_y-excitation RR spectra of RCs are difficult to obtain owing both to the intrinsic fluorescence from P* (quantum yield ~0.004; Zankel et al., 1968) and to the fluorescence from exogenous BChl pigments (quantum yield ~0.15; Becker et al., 1991) present in very small amounts in the RC preparation. Donohoe et al. (1990) reported the first Q_y-excitation RR spectra of P. These spectra were obtained at low temperature (12 K) and were limited to a relatively narrow region of the low-frequency regime (70–220 cm^{-1}). These workers identified with certainty only two RR bands (~102 and ~138 cm^{-1}) superimposed on the fluorescence background. More recently, Shreve et al. (1991) reported near-ambient temperature (278 K) Q_y-excitation RR spectra of P. These workers observed very weak RR bands (~0.1% of the total intensity) on a large fluorescence background and resorted to a difference technique which is a modification of the excitation frequency shifting method developed by Funfschilling and Williams (1976) to delineate the underlying RR signals. In the original technique,

† This work was supported by Grants GM39781 (D.F.B.) and GM30353 (H.A.F.) from the National Institute of General Medical Sciences.

‡ University of California.

§ University of Connecticut.

[1] Abbreviations: BChl, bacteriochlorophyll; CCD, charge coupled device; DEAE, (diethylamino)ethyl; FT, Fourier transform; L and M, light and medium polypeptides, respectively, of the reaction center; P, special pair; RR, resonance Raman; RC, reaction center; Tris, tris-(hydroxymethyl)aminomethane.

0006-2960/92/0431-11050$03.00/0

the excitation wavelength is rapidly modulated and the spectra acquired at the two wavelengths are subtracted to eliminate the background. In the experiments of Shreve et al. (1991), RR spectra were collected for extended periods (20–40 min) at one excitation wavelength; the excitation wavelength was then shifted by 10–25 cm^{-1} and a second data set was obtained. Subsequent subtraction and least-squares fitting yielded the RR data. The utility of both this and the original method is pinned on the assumption that the backgrounds in the two data sets are essentially identical across the spectral window. Using this technique, Shreve et al. (1991) examined the 30–1800-cm^{-1} region and observed several RR difference bands. In the low-frequency region, bands were observed at 94 and 127 cm^{-1} that probably correspond to the 102 and 138 cm^{-1} bands reported by Donohoe et al. (1990). Low-frequency bands were also observed at 36, 71, 202, and 337 cm^{-1}. Only three bands were observed in the 650–900-cm^{-1}, region and no bands of substantial intensity were observed above 900 cm^{-1}. The dearth of strong RR bands in the higher-frequency regime, particularly in the 900–1800-cm^{-1} region, is puzzling given that Q_y-excitation RR spectra of BChl model compounds exhibit a large number of bands throughout the 200–1800-cm^{-1} range (Donohoe et al., 1988). Preresonant Fourier transform (FT) Raman spectra of RCs acquired with 1064-nm excitation also exhibit a large number of bands characteristic of BChl in this spectral region (Mattioli et al., 1991; Johnson & Rubinovitz, 1990, 1991; Noguchi et al., 1991). Many of the bands observed in the FT–Raman spectra are clearly due to scattering from P as might be expected because 1064-nm excitation is energetically much closer to the Q_y absorption of P than to the Q_y absorptions of the other pigments in the RC. Thus, the general characteristics of the FT–Raman spectra of RCs suggest that the scattering from P is more or less typical of that observed for tetrapyrrolic macrocycles (Lutz, 1984; Lutz & Robert, 1988; Lutz & Mäntele, 1991; Schick & Bocian, 1987).

In attempts to gain a clear understanding of the RR scattering characteristics of P, we have performed a detailed Q_y-excitation RR study of RCs from *Rhodobacter sphaeroides* 2.4.1. The excitation wavelengths used in this study range from 800 to 920 nm, and the spectral windows include both the low- and high-frequency scattering regimes. RR data were also obtained at low and high temperatures (25 and 201 K) in order to determine whether temperature has a significant effect on the characteristics of the RR scattering. Spectra were obtained both in a normal fashion (Donohoe et al., 1990) and via the difference technique used by Shreve et al. (1991) in order to compare these two schemes of data acquisition. All of these RR data were acquired with a signal-to-noise ratio that is 10–20 times better than that of our preliminary study (Donohoe et al., 1990). Plausible vibrational assignments are also suggested for the low-frequency (30–500 cm^{-1}) vibrations of both P and the accessory BChls on the basis of semiempirical normal coordinate calculations. Collectively, these data provide new insights into the nature of the RR scattering from P. The characteristic features of the RR scattering have important implications for the initial charge-separation event in bacterial photosynthesis.

MATERIALS AND METHODS

Experimental Procedures. The RCs from *Rb. sphaeroides* 2.4.1 were prepared as previously described (McGann & Frank, 1987). The proteins were eluted from a DEAE anion-exchange column by using 0.01 M Tris (pH 8.0), 0.015% Triton X-100, and 0.5 M NaCl. The RCs were chemically reduced or oxidized by adding an excess of $Na_2S_2O_4$ or $K_3Fe(CN)_6$, respectively.

The RR measurements were made on glassed samples (~1:1 in ethylene glycol, total concentration ~28 μM) contained in a 1-mm-i.d. capillary tube. Temperature control was achieved by mounting the sample on the cold tip of a closed cycle refrigeration system (ADP Cryogenics DE-202 Displex), via a home-built holder. The scattering was collected in a 90° configuration by using a 0.6-m triple spectrometer (Spex Industries 1877). A liquid nitrogen cooled (−120 °C) charge coupled device (CCD) served as the detector (Princeton Instruments LN/CCD equipped with an antireflection coated, back-illuminated 512 × 512 pixel Tektronix chip). This CCD has a quantum efficiency of ~50% at 850 nm and ~20% at 1000 nm. The excitation wavelengths in the 800–920-nm region were provided by the output of a Ti–sapphire laser (Coherent 890) pumped by the visible multiline output of an argon ion laser (Coherent Innova 400). The laser power levels at the sample were typically 0.3–1 mW. The beam was defocused to illuminate a volume of 1–2 μL. The resulting photon flux of ~100 photons/(s·RC) is sufficiently low that less than 2% of the RCs exist in photogenerated transient states such as P^+ or ^3P at any of the excitation wavelengths used. In order to further preclude the possibility of photodegradation, the samples were repositioned in the laser beam after every scan. Even a small amount of photodamage is discernible in the RR experiment because the loss of sample integrity leads to a significant increase in the level of spurious fluorescence. The RR spectra shown were obtained by coadding 4–10, 1-h (30 × 120 s) scans. Cosmic spikes in the individual data sets were removed prior to coaddition. Typical slit widths used in the RR experiments yielded a resolution of 1–4 cm^{-1} depending on the excitation wavelength and/or the spectral region in the data acquisition window.

The RR signals are superimposed on a large fluorescence background; however, the signals are clearly visible and exhibit intensities that are in the range 1–5% of the total signal intensity. This level of RR signal intensity allows background removal via subtraction of a standard polynomial fit to the broad-band emission. Prior to background subtraction, the spectra were flat field corrected by using a spectrally broad emission lamp. The relative RR intensities are extremely sensitive to the details of the polynomial fitting procedure; consequently, the relative intensities are accurate to no better than ±50%. The RR frequencies are also sensitive to the details of the fitting procedure. The frequencies are accurate to ±3 cm^{-1} for strong and isolated bands and ±6 cm^{-1} for weak and overlapping bands. Unless otherwise stated, the spectra presented were smoothed via a 5-point Savitsky–Golay algorithm. Difference RR spectra were acquired as described by Shreve et al. (1991). Data sets acquired with the exciting line shifted by small wavenumber increments (10–25 cm^{-1}) were compared in order to assess whether detector intensity artifacts were present; no significant artifacts could be identified. The vibrational frequencies obtained by either technique were calibrated using the known frequencies of CCl_4 and indene.

In the course of the experiments, we attempted to quantitate the RR intensities via comparison with an internal intensity standard. Raman scattering could not be observed from either the solvent or buffer under the extremely low photon flux densities used in the RR experiments; consequently, various water-soluble compounds (such as Na_2SO_4) were added to the sample in attempts to obtain an internal intensity standard. However, quantitative intensity calibration was precluded

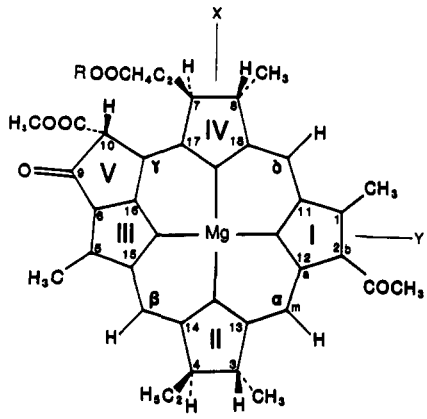

FIGURE 1: Structure and labeling scheme for the BChl molecule.

because none of the known intensity standards exhibited observable scattering under the conditions of the RR experiments. In order to obtain a qualitative estimate of the relative RR intensities observed with different excitation wavelengths, the spectra of the RCs were compared to the Raman spectra of CCl_4 (low-frequency region) or indene (mid- and high-frequency region). The Raman spectra of the external standards were obtained under identical conditions at the different excitation wavelengths. Repeated acquisitions of the RR spectra of RCs versus the Raman spectra of the standard at a given excitation wavelength indicated that the precision of this intensity measurement is ±50%.

Normal Coordinate Calculations. The calculated vibrational frequencies and normal coordinates for the low-frequency modes of BChl were obtained by using the QCFF/PI method (Warshel & Karplus, 1972; Warshel & Levitt, 1974). The calculations were performed as previously described in our analysis of the high-frequency vibrations of Cu(II)–bacteriopheophytin *a* (Donohoe et al., 1988). In the present calculations, the Cu(II) atom was replaced by Mg(II) and the C_2 acetyl group was explicitly included (the labeling scheme is illustrated in Figure 1). The methyl group of the acetyl fragment was treated as a point mass of 15 amu.

RESULTS

RR Spectra of Reduced RCs. Low-frequency (40–430 cm^{-1}) RR spectra of chemically reduced RCs at 201 K obtained with excitation at 800, 825, 851, 872, and 896 nm are shown in Figure 2. Spectra were also obtained at 810 and 916 nm (not shown); however, these spectra do not reveal any features in addition to those shown in Figure 2. The RR spectra at all excitation wavelengths reveal the presence of a number of bands (at least 20). Spectra obtained with λ_{ex} = 872 and 896 nm (near and to the red, respectively, of the absorption maximum of P) clearly show 105- and 138-cm^{-1} bands as previously reported by Donohoe et al. (1990). Low-frequency bands are also observed near 51, 80, 216, and 340 cm^{-1} which may correspond to the 36, 71, 202, and 337-cm^{-1} bands reported by Shreve et al. (1991). However, unlike the RR spectra reported by the latter workers, our spectra exhibit other bands in the 200–430-cm^{-1} region. In particular, bands are observed near 237, 250, 293, 310, 360, and 407 cm^{-1}. Bands are also observed near these frequencies in the 1064-nm-excitation FT–Raman spectra (Johnson & Rubinovitz, 1990, 1991). In these latter spectra as well as in ours, many of the bands are relatively weak in comparison with the ~340-cm^{-1} band. However, this is not the case for the 293- and 360-cm^{-1} bands. Both of these bands appear as distinct satellites on the 340-cm^{-1} band. As the excitation wavelength

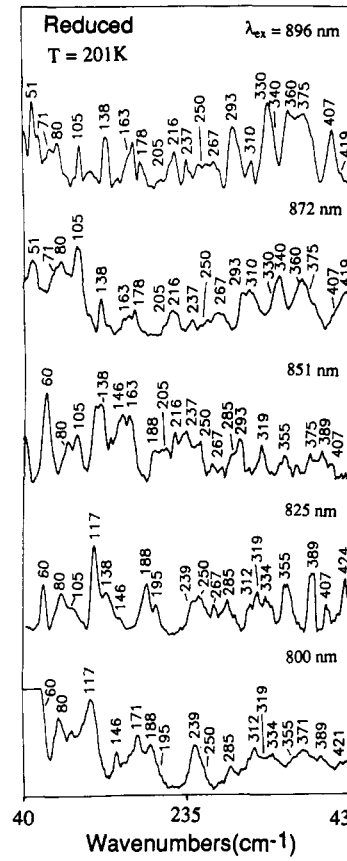

FIGURE 2: Low-frequency RR spectra of reduced RCs from *Rb. sphaeroides* 2.4.1 at 201 K with λ_{ex} = 896, 872, 851, 825, and 800 nm. The relative intensities of the different spectra shown do not correspond to the actual values but are scaled for pictorial clarity (see text).

is tuned to the blue side of the absorption band of P, new bands are observed in the RR spectrum. For example, with λ_{ex} = 851 and 825 nm, bands are observed at 60, 117, 146, and 188 cm^{-1} that are not observed with λ_{ex} = 896 or 872 nm. These bands are attributable to scattering from the accessory BChl pigments (Lutz, 1984; Lutz & Robert, 1988; Lutz & Mäntele, 1991) that gains intensity as the excitation wavelength approaches the Q_y absorption band(s) of these pigments (λ_{max} ~ 805 nm). With excitation at λ_{ex} = 825 and 800 nm, the bands of the BChls dominate the RR spectra. In order to determine whether all of the low-frequency modes observed with excitation energies resonant with P* are in fact due to P, RR spectra were also acquired for chemically oxidized samples. Figure 3 compares the RR spectra of oxidized RCs obtained with λ_{ex} = 872 and 800 nm. The relative scales of the two spectral traces shown in this figure are the same as those shown in Figure 2. As can be seen, no Raman scattering is observed from the oxidized samples with λ_{ex} = 872 nm, whereas appreciable scattering is observed with λ_{ex} = 800 nm. [It should be noted that the extremely low laser powers used in all the RR experiments precludes the observation of preresonance Raman scattering from the other pigments in the RC with λ_{ex} = 872 nm.] Comparison of the spectra of the reduced and oxidized RCs obtained with λ_{ex} = 872 nm reveals that the accessory BChls are affected by oxidation of P (vide infra).

RR spectra of reduced and oxidized RCs were also obtained in the 430–1800-cm^{-1} region. In contrast to the report of Shreve et al. (1991), the RR spectra of reduced RCs exhibit a number of RR bands at all excitation wavelengths. This is illustrated in Figures 4–6 which show portions of the spectra

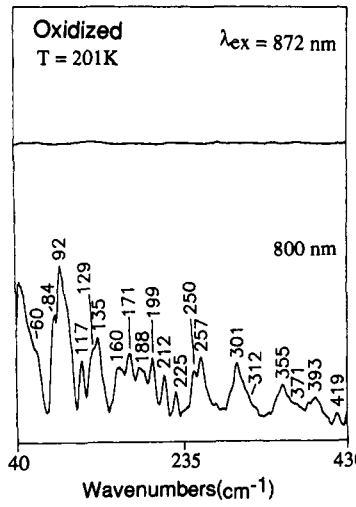

FIGURE 3: Low-frequency RR spectra of oxidized RCs from *Rb. sphaeroides* 2.4.1 at 201 K with λ_{ex} = 872 and 800 nm. The relative intensities of the two spectra shown do not correspond to the actual values but are scaled for pictorial clarity. The relative intensities are, however, identical to those shown for the analogous spectra in Figure 2 (see text).

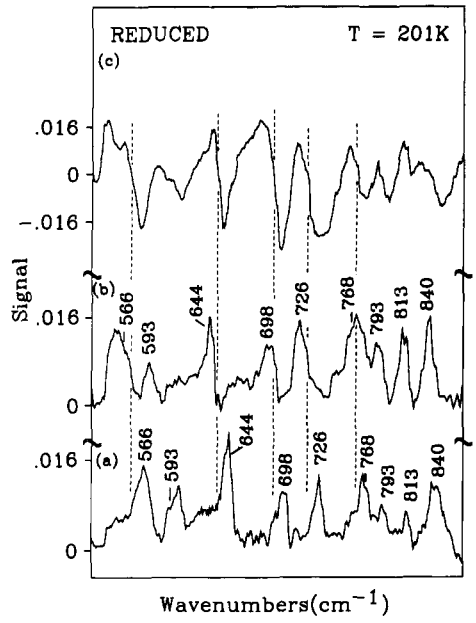

FIGURE 4: Mid-frequency RR spectra of reduced RCs from *Rb. sphaeroides* 2.4.1 at 201 K. (a) Flat-field corrected, background subtracted spectrum obtained with λ_{ex} = 872 nm. (b) Same as (a) but with λ_{ex} shifted by 16 cm^{-1}. Note that the spectra shown in (a) and (b) are plotted on an absolute wavenumber scale whereas the frequencies of the labeled RR bands are given as wavenumber shifts from λ_{ex}. (c) Difference spectrum obtained by subtracting the data sets used to generate the spectra shown in (a) and (b) but without flat-field correction or background subtraction (see text). Representative difference features for relatively isolated bands are marked by dashed lines. None of the spectra shown are smoothed.

obtained in the mid- and high-frequency regions. The specific features of these spectra are discussed in more detail below.

The flat-field corrected, background subtracted RR spectrum in the 535–875-cm^{-1} region obtained with λ_{ex} = 872 nm is shown in Figure 4a. The flat-field corrected, background subtracted spectrum in the 1200–1430-cm^{-1} region obtained with λ_{ex} = 885 nm is shown in Figure 5a. Bands of appreciable intensity are observed in the former spectrum near 566, 644, 698, 726, and 768 cm^{-1} and in the latter near 1217, 1227, 1265, and 1292 cm^{-1} (a cluster of modes is observed in the 1300–1430-cm^{-1} region). All of these features bleach upon

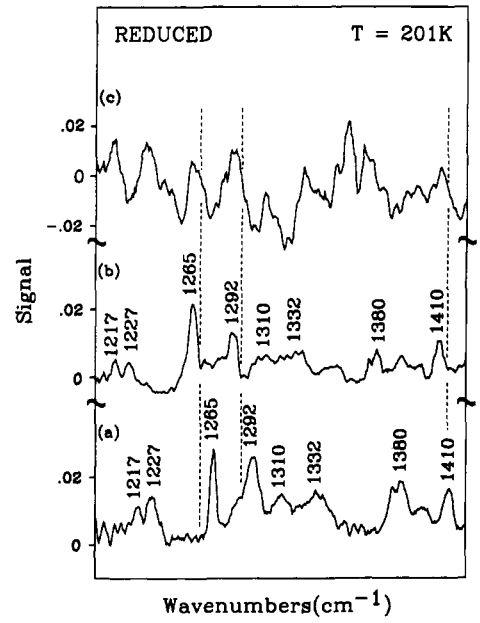

FIGURE 5: High-frequency RR spectra of reduced RCs from *Rb. sphaeroides* 2.4.1 at 201 K. (a) Flat-field corrected, background subtracted spectrum obtained with λ_{ex} = 885 nm. (b) Same as (a) but with λ_{ex} shifted by 11 cm^{-1}. Note that the spectra shown in (a) and (b) are plotted on an absolute wavenumber scale whereas the frequencies of the labeled RR bands are given as wavenumber shifts from λ_{ex}. (c) Difference spectrum obtained by subtracting the data sets used to generate the spectra shown in (a) and (b) but without flat-field correction or background subtraction (see text). Representative difference features for relatively isolated bands are marked by dashed lines. None of the spectra shown are smoothed.

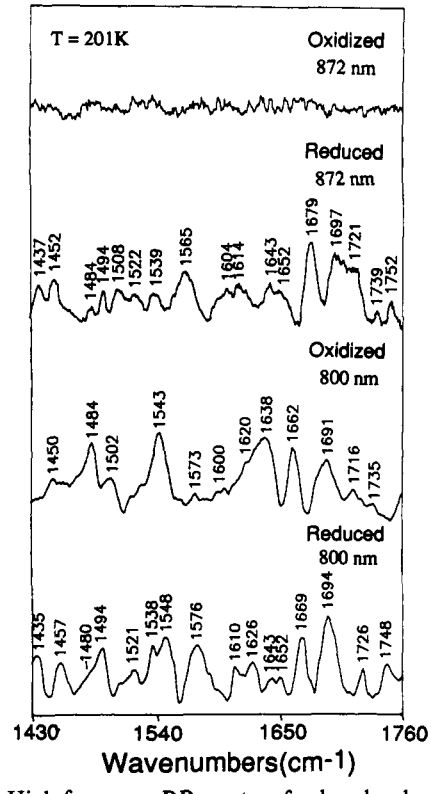

FIGURE 6: High-frequency RR spectra of reduced and oxidized RCs from *Rb. sphaeroides* 2.4.1 at 201 K with λ_{ex} = 872 and 800 nm.

oxidation of P (not shown). In contrast, the spectrum reported by Shreve et al. (1991) exhibits only two bands in the lower wavenumber region, a strong feature at 728 cm^{-1} and a weaker feature near 685 cm^{-1} and no bands of appreciable intensity in the higher wavenumber regime. The flat-field corrected,

background subtracted spectra obtained after a small shift in the excitation wavelength are shown in Figures 4b and 5b. The flat-field correction used for the data set shown in Figure 4b (Figure 5b) is the same as that used for the data set shown in Figure 4a (Figure 5a), whereas the background subtraction is different. The general features observed in the spectra shown in spectrum a in Figure 4 (Figure 5a) and spectrum b in Figure 4 (Figure 5b) are quite similar; however, the frequencies and relative intensities of the RR bands are not identical in the two data sets due to the intrinsic limitations in the reproducibility of the data and to differences in the background subtraction (vide supra). The difference spectrum obtained by subtracting the data sets of spectrum a in Figure 4 (Figure 5a) and spectrum b in Figure 4 (Figure 5b) without flat-field correction or background subtraction is shown in Figure 4c (Figure 5c). As is evident, all of the spectral features observed in the flat-field corrected, background subtracted spectra are observed in the uncorrected, unsubtracted difference spectra. This result indicates that none of the features observed in the RR spectra are due to artifacts of the flat-field correction or background subtraction.

The high-frequency (1430–1760 cm^{-1}) RR spectra obtained with λ_{ex} = 872 and 800 nm are compared in Figure 6. The oxidation-induced bleaching of the high-frequency bands observed with λ_{ex} = 872 nm clearly indicates that these bands are due to P. The observation of a large number of high-frequency RR bands due to P is consistent with 1064-nm excitation FT–Raman studies of RCs (Mattioli et al., 1991; Johnson & Rubinovitz, 1990, 1991; Noguchi et al., 1991). Indeed, many of the high-frequency RR bands observed with λ_{ex} = 872 nm can be correlated with structure-sensitive modes previously identified in the RR spectra of P (Lutz, 1984; Lutz & Robert, 1988; Lutz & Mäntele, 1991; Mattioli et al., 1991). For example, bands are observed at 1697 and 1679 cm^{-1} that correspond to the C_9 keto carbonyl stretching modes of P_L and P_M. A pair of bands is also observed at 1643 and 1652 cm^{-1} which are probably due to the C_2 acetyl carbonyl stretching modes of these two pigments, respectively (although a frequency of 1643 cm^{-1} is higher than that previously reported for ν(C=O) of the C_2 acetyl group of P_L; Mattioli et al., 1991). Interestingly, at least two bands are observed in the region of the ν_{10}-like mode, one near 1614 cm^{-1} and the other near 1604 cm^{-1}. The former band occurs at a frequency typical of a five-coordinate BChl (Lutz, 1984; Lutz & Robert, 1988), whereas the latter is somewhat lower. Crystallographic studies on RCs indicate that the Mg–histidine bond of P_M is typical in length and much shorter than that of P_L (El-Kabbanni et al., 1991; Yeates et al., 1988). These data in conjunction with the RR results suggest that the 1614-cm^{-1} and 1604-cm^{-1} bands can be attributed to P_M and P_L, respectively.

In order to investigate the relative RR intensities at the various excitation wavelengths, a qualitative RR excitation profile (not shown) was constructed by using the external CCl_4 and indene standards. This profile indicates that the average RR intensity observed upon excitation into the Q_y-absorption band of P approximately follows the band contour as reported by Shreve et al. (1991). [The average RR intensity was used because the intensities of individual bands could not be determined reliably (vide supra).] In addition, the average RR intensity observed for the low-frequency modes with λ_{ex} = 872 nm appears to be ~5–15 times *greater* than that observed with λ_{ex} = 800 nm. This intensity difference is nominally outside the error limits measured for the external standard method of determining the relative intensities. These results suggest that the RR scattering from the low-frequency modes of P is significantly stronger than that for these modes of the accessory BChls. In the case of the high-frequency modes, the average RR intensity observed with λ_{ex} = 872 nm also appears to be greater than that observed with λ_{ex} = 800 nm; however, this difference is not nearly as large as that observed for the low-frequency modes. [It should be noted that the lower signal-to-noise ratio apparent in the former spectrum vs the latter in Figure 6 is due to the diminished detector response at the longer detection wavelengths.]

The question remains as to why the RR spectra of P reported by Shreve et al. (1991) show far fewer bands than those reported in this study or in the FT–Raman studies. In the case of the high-frequency modes, this discrepancy is probably due to the relatively low sensitivity above 1000 nm of the front-illuminated CCD used in their experiments. The fact that the front-illuminated CCD is in general much less red-sensitive than the back-illuminated device used in our experiments probably also contributes to Shreve et al.'s (1991) failure to observe weak and moderately intense bands in the mid- and low-frequency regions. Regardless, differences in signal-to-noise alone cannot explain all of the discrepancies between their spectra and ours. For example, we observe bands at 566, 644, and 726 cm^{-1} with λ_{ex} = 872 nm which all appear to be of comparable intensity (Figure 4), whereas Shreve et al. (1991) observe a single band at 728 cm^{-1} with λ_{ex} = 850 nm. On the basis of the signal-to-noise ratio Shreve et al. (1991) observe for the ~730-cm^{-1} band, both the 566- and 644-cm^{-1} bands should also be observed. The fact that they are not suggests that relative intensities of these latter bands versus the ~730-cm^{-1} band are different (by at least a factor of 2) in their RR spectra versus ours. The factors that contribute to these differences between the spectra are not certain. However, it should be noted that the excitation wavelengths, temperatures, and sample conditions are not identical in our experiments and those of Shreve et al. (1991). Differences in temperature and/or sample condition might also account for the apparent frequency differences between bands observed in common between the two sets of experiments (vide supra).

Effects of Oxidation on the RR Spectra. The most obvious effect of oxidation of the RR spectra is the bleaching of the bands due to P. However, with λ_{ex} = 872 nm, extremely weak features are discernible in the spectra of oxidized RCs. We originally attributed these bands to scattering by small amounts of unoxidized RCs. However, preliminary RR experiments conducted at much higher laser powers (~35 mW) indicate that the bands are not at the same frequencies as those observed for reduced RCs. Preliminary high-frequency RR data obtained with high laser powers suggest that these bands may in fact be due to scattering by P^+.

Examination of the low- and high-frequency RR spectra of oxidized RCs obtained with λ_{ex} = 800 nm clearly reveals that formation of P^+ induces changes in the RR spectra of one or both of the accessory BChls. Oxidation-induced changes in the high-frequency RR spectra of the accessory BChls have previously been observed by using B-state excitation. For example, Robert and Lutz (1988) have reported that $\nu(C_9{=}O)$ of $BChl_L$ downshifts upon oxidation of P whereas the analogous mode of $BChl_M$ is unaffected. The oxidation-induced changes observed in the Q_y-excitation RR data are qualitatively consistent with this result (Figure 6). In particular, the bands due to the $\nu(C_9{=}O)$ modes of $BChl_L$ and $BChl_M$ in reduced RCs are overlapped and occur near 1694 cm^{-1}. Upon oxidation, the centroid of the band contour appears to downshift by ~3 cm^{-1} and a distinctive shoulder appears on

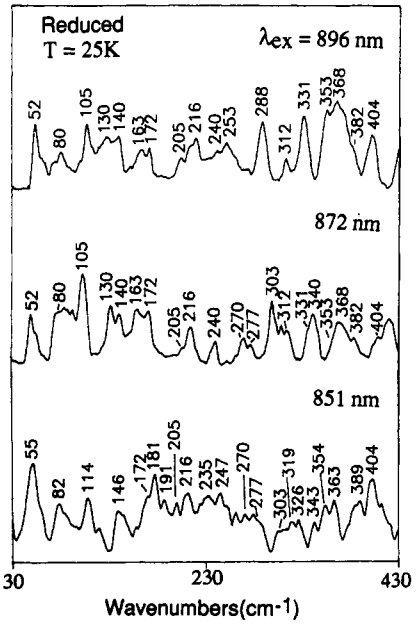

FIGURE 7: Low-frequency RR spectra of reduced RCs from *Rb. sphaeroides* 2.4.1 at 25 K with λ_{ex} = 896, 872, and 851 nm. The relative intensities of the different spectra shown do not correspond to the actual values but are scaled for pictorial clarity (see text).

the low-frequency side of the band. In the B-state-excitation RR studies, the oxidation-induced changes in the ν(C=O) modes of the C_2 acetyl groups are less clear. The bands due to these modes of the two accessory BChls are overlapped and are observed near 1669 cm^{-1} in the Q_y-excitation RR spectra reported here (Figure 6). Upon oxidation of the RCs, this band appears to downshift by $\sim$7 cm^{-1} and a shoulder remains on the high-frequency side. This result suggests that the C_2 acetyl group of one of the accessory BChls (most likely $BChl_L$) also shifts upon formation of P^+. Other oxidation-induced shifts are discernible in the Q_y-excitation RR spectra of the accessory BChls; however, the exact nature of the spectral changes must await a detailed analysis of the data.

Effects of Temperature on the RR Spectra of Reduced RCs. The low-frequency Q_y-excitation RR spectra of reduced RCs with λ_{ex} = 896, 872, and 851 nm obtained at 25 K are shown in Figure 7. Comparison with Figure 2 reveals that lowering the temperature from 201 K to 25 K does not in general result in large changes in the RR spectra. In particular, none of the bands observed in the higher temperature RR spectrum disappear upon cooling. This result indicates that none of the low-frequency bands observed at 201 K are due to a difference mode that arises as a result of thermal population of higher-lying vibrational states. In general, the spectra obtained at 25 K do not exhibit any additional bands. A clear exception is the appearance of a doublet at 130 and 140 cm^{-1} instead of the single band observed at 138 cm^{-1} at 201 K (cf. Figures 2 and 7). Another interesting point concerns the RR intensity enhancement patterns observed at 25 K vs 201 K. At low temperature, the spectrum observed with λ_{ex} = 851 nm appears to be primarily due to the accessory BChls as is evidenced by the appearance of bands at 114 and 146 cm^{-1}. In contrast, at 201 K scattering from P dominates with this excitation wavelength. These changes in the general appearance of the RR spectra can be attributed to the fact that the Q_y absorption maximum of P red shifts by several hundred wavenumbers upon cooling from 201 K to 25 K (Kirmaier & Holten, 1988). This temperature-induced absorption shift diminishes the RR scattering intensity from P with λ_{ex} = 851 and allows bands due to the accessory BChls to become clearly visible.

Vibrational Assignments for the Low-Frequency Modes. The low-frequency RR spectra acquired of both P and the accessory BChls exhibit a large number of bands. The frequencies of the bands observed for the two different pairs of pigments are not identical. This is not surprising because the frequencies of tetrapyrrolic macrocycle modes in this region are very sensitive to the conformation of the ring (Li et al., 1989). In this regard, X-ray crystallographic studies indicate that the conformations of the various BChl rings in RCs are different (Chang et al., 1986; Allen et al., 1986). In addition, the Mg–histidine bond lengths of $BChl_L$ and $BChl_M$ are different from one another as are those of P_L and P_M (Allen et al., 1988; Yeates et al., 1988; El-Kabbani et al., 1991). Accordingly, one might expect the RR spectra of both P and the accessory BChls to be comprised of two sets of bands. Depending on the sensitivity of the frequency of a particular mode to the conformation of the ring, the bands due to P_L and P_M ($BChl_L$ and $BChl_M$) may or may not be within the bandwidth. In the case of P, the situation is further complicated by the potential effects of electronic coupling between the two closely spaced macrocycles. If a particular vibration of the BChls in P is strongly coupled to the electronic transition, it might be expected that only the symmetrical linear combination of the modes is strongly RR active. For less strongly coupled modes, relatively weak RR bands due to the two BChls in P might appear in the RR spectra. The complexity of the low-frequency RR spectra of both P and the accessory BChls precludes an analysis of the spectra in terms of the various possibilities discussed above. Despite these uncertainties in the characterization of the RR spectra, inspection of Figure 2 reveals that most of the RR bands observed for P can be correlated with those observed for the accessory BChls. These correlations are presented in Table I. If indeed a one-to-one correspondence exists for the RR bands of P and the accessory BChls, then all the RR bands of P are due to fundamental vibrations of the BChls that constitute the $BChl_2$ unit.

In order to gain a more quantitative understanding of the nature of the low-frequency vibrational modes, semiempirical normal coordinate calculations were conducted on the BChl molecule. The results of these calculations are included in Table I. The calculations predict that at least 50 vibrational modes occur below 500 cm^{-1}. This is far greater than the number of bands observed in the RR spectrum. However, inspection of the normal-mode compositions indicates that many of these vibrations are due to deformations of the nonconjugating substituent groups. These modes are expected to exhibit far less RR intensity enhancement than skeletal modes of the BChl ring (Li et al., 1989). If these modes are excluded as possible contributors to the RR spectra, then a plausible set of vibrational assignments can be made for the low-frequency RR bands of the BChls in the RCs. A suggested set of assignments is given in Table I. Inspection of the table reveals that all but one of the modes below 200 cm^{-1} are out-of-plane deformations whereas those in the 200–500-cm^{-1} range are primarily in-plane modes. (The distinction between in-plane and out-of-plane is only qualitative because the macrocycle is not planar; Chang et al., 1986; Allen et al., 1986.) Most of the normal coordinates are quite complicated in appearance and contain contributions from a large number of internal coordinates.

Table I: Observed (RR) and Calculated Low Frequency Modes of BChl and $BChl_2$

obsd		calcd	
$BChl_2$[a]	BChl[b]	BChl	description[c]
		498	δ ring II, IV
		488	$\delta C_{acetyl}CH_3$, $\delta C_{acetyl}O$
		480	$\delta C_{acetyl}CH_3$, $\delta C_{acetyl}O$
468	468	459	γ ring I, IV (swivel)
		451	δC_bC_{alkyl}(III), δC_9O
448	448	440	γ ring I, IV (swivel, tilt), δC_9O
431	434	420	γ ring I, IV (swivel, tilt), δC_bC_{alkyl} (III)
~412[d]		399	γ ring III (swivel, tilt), γ ring V
	389	393	$\delta C_{acetyl}O$, $\delta C_{acetyl}CH_3$, γC_bC_{alkyl} (III)
		387	γ ring V
		372	$\delta C_{acetyl}CH_3$, δC_bC_{alkyl} (III)
375	371	370	γ ring I (swivel, tilt)
		351	γ ring II (fold, tilt), δC_bC_{alkyl} (I)
		343	γ ring IV (fold, tilt), δC_bC_{alkyl} (III), νMgN
360	355	338	νMgN, δC_bC_{alkyl} (II, IV)
		334	δC_bC_{alkyl} (II, IV), νMgN
		329	δC_bC_{alkyl} (II, III), δC_9O, νMgN
~335[d]	334	326	νMgN, δC_bC_{alkyl} (II, III)
	319	320	$\delta C_{10}C_{carbo}$, δC_bC_{alkyl} (III, IV)
310	312	299	νMgN, $\delta C_{acetyl}CH_3$
		291	$\gamma C_aC_m(\alpha,\beta)$, γ ring I (tilt)
293	285		
		279	νMgN, δC_bC_{alkyl} (III)
~267[d]		270	$\delta C_{acetyl}O$, δC_bC_{alkyl} (III)
		263	γC_aC_m (β, δ), νMgN
250		260	γC_aC_m (α, β, δ), νMgN
		256	$\delta C_{10}C_{carbo}$, νMgN, $\delta C_{acetyl}O$
237	239	235	δC_bC_{alkyl} (II, IV), γ ring I (tilt)
216		218	$\delta C_{10}C_{carbo}$, δC_9O, δC_bC_{alkyl} (IV)
205	195	200	δC_bC_{alkyl} (II), δC_2C_{acetyl}
		191	δC_bC_{alkyl} (IV)
		186	δC_bC_{alkyl} (II, IV)
		173	δC_bC_{alkyl} (II), $\delta C_{10}C_{carbo}$
		169	γC_bC_{alkyl} (II, IV), $\delta C_{10}C_{carbo}$
178	188	162	γMgN, δC_bC_{alkyl} (II, IV)
163	171	146	γMgN, δC_9O, $\delta C_{10}C_{carbo}$
138	146	141	δC_2C_{acetyl}
		129	γC_bC_{alkyl} (I, III), γC_aC_m (α,β,δ)
105	117	109	γMgN, γC_aC_m (α,β)
		91	γC_bC_{alkyl} (III), $\gamma C_{10}C_{carbo}$
~75[d]	~80[d]	78	γMgN, $\gamma C_{10}C_{carbo}$
		70	γC_bC_{alkyl} (I, III, IV), $\gamma C_{10}C_{carbo}$, γMgN
51	60	61	γ ring I (translation)
		53	γC_bC_{alkyl} (II, III, IV)
		36	acetyl torsion, γC_bC_{alkyl} (I, III)
		32	acetyl torsion, γC_bC_{alkyl} (I, III)
		26	γC_2C_{acetyl}, γC_bC_{alkyl} (III)
		20	γ ring III, V (translation)

[a] Observed with λ_{ex} = 872 nm at 201 K. [b] Observed with λ_{ex} = 800 nm at 201 K. [c] Mode descriptions are as follows: ν = stretch, δ = in-plane deformation, and γ = out-of-plane deformation. The designators C_a, C_b, C_m, I-IV, α, β, and δ refer to Figure 1. For descriptions of tilt, fold, swivel, and translation, see Li et al. (1989). [d] Multiple bands occur in this region, and the listed frequency is an average value.

DISCUSSION

The RR spectra reported herein provide insight into the vibrational and electronic structure of both P and the accessory BChls in RCs. The RR spectra of both types of pigments are extremely rich and exhibit numerous bands in both the low- and high-frequency regions. In this respect, these pigments are similar to other tetrapyrrolic macrocycles (Schick & Bocian, 1987). It is noteworthy that the RR spectrum of P exhibits the full complement of vibrational bands which can in general be correlated with those observed for the accessory BChls. The low-frequency RR spectra of P are of particular interest. Second-derivative absorption (Klevanik et al., 1988) and hole-burned (Johnson et al., 1989, 1990) spectra have been modeled in terms of one or a few vibronically active low-frequency modes with very large Huang–Rhys factors

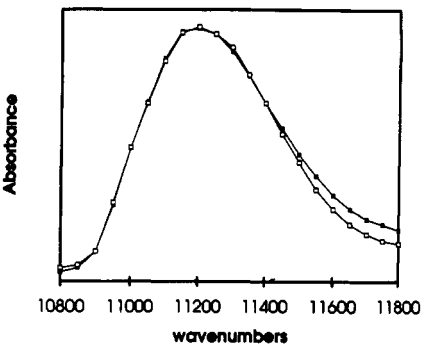

FIGURE 8: Observed (open squares) and calculated (closed squares) Q_y-absorption band of P in RCs from *Rb. sphaeroides* 2.4.1. The observed spectrum was acquired at 4.2 K in a glycerol glass. The calculated spectrum was obtained by using the following frequencies (*S* values): 52 (0.30), 80 (0.23), 105 (0.63), 130 (0.43), 140 (0.43), 163 (0.06), 172 (0.07), 216 (0.05), 253 (0.04), 288 (0.03), 331 (0.03), 353 (0.02), 368 (0.02), 404 (0.01), 468 (0.01), 566 (0.02), 593 (0.01), 644 (0.03), 698 (0.03), 726 (0.03). The system origin is at 11 000 cm^{-1}, and the inhomogeneous width is 140 cm^{-1}.

(*S*). These modes have been suggested to be special vibrations unique to P rather than modes derived from monomer-like vibrations (Warshel, 1980). The RR spectra reported here indicate that the actual interpretation is more complex than previously believed. Many low-frequency modes are vibronically active and all of these can probably be attributed to monomer-like vibrations (albeit, they may be coupled monomer-like vibrations which gain significant Franck–Condon activity only because of the electronic coupling between the constituent BChls in P) rather than to vibrations arising from the additional degrees of freedom present in the dimer. There is no definitive evidence for an overtone progression in any mode that would signify an extremely large displacement along a particular coordinate (Myers & Mathies, 1987). Collectively, these data suggest that the vibronic progressions observed in the second-derivative and hole-burned spectra represent the effective frequencies of numerous overlapping bands rather than the actual frequencies of one or two modes.

Although the number and frequencies of the RR bands of P are similar to those of the accessory BChls, the RR intensities exhibited by the two types of BChls in RCs are quite different. The low-frequency modes of P are unusually strong assuming that these modes of the accessory BChls exhibit normal RR intensities. This observation suggests that a number of the low-frequency modes of P are strongly coupled to the electronic transition and no single mode is dominant. [It should be emphasized that the RR cross-sections are determined by the magnitude of the electronic transition–dipole moments and the vibronic relaxation times in addition to the vibrational overlaps (Myers & Mathies, 1987). The relative contribution of each of these factors to the RR intensities of the modes of P versus those of the accessory BChls is not known.] In attempts to gain a more quantitative picture of the magnitude of the electron–phonon coupling for the various vibrational modes, we simulated the Q_y absorption band of P at low temperature. The results of this simulation are shown in Figure 8. The calculation was performed by including the 15 prominent modes observed in the RR spectra below 500 cm^{-1} and five other modes observed in the 500–750-cm^{-1} range (see Figure 6). The calculation is not exact because only transitions involving 5 quanta or less are included. The *S* values for the various modes were constrained such that their magnitudes were not allowed to become large enough that overtones should be obviously visible in the RR spectra. In particular, *S* was held to a value less than 0.5 although the simulations indicate that at least one mode with an *S* somewhat

larger than this value is required to fit the spectra. The exact S values used in the simulation are given in the legend of Figure 8. The large number of parameters included in the simulation allows a reasonable fit of the absorption contour. Although the fit is not unique, the frequency distribution of the vibronically active modes places certain constraints on the average S values of the modes whose frequencies fall above and below 200 cm^{-1}. In particular, fewer modes occur in the 30–200-cm^{-1} range than in the 200–750-cm^{-1} region. The low-quantum vibronic satellites of the former modes contribute to the red side of the absorption contour. The smaller number of modes in the lower frequency regime dictates that the average S is larger ($\sim$0.30) than that of the modes in the range 200–750 cm^{-1} (<0.05). [If modes below 30 cm^{-1} (the lower limit of our RR measurements) also contribute to absorption contour, then the average S of the observed low-frequency modes will be smaller.] Finally, it should be noted that the observed near-normal intensity scattering from high-frequency modes of P indicates that vibronic satellites of these modes must also contribute to the absorption contour. These satellites should be relatively weak and outside the band normally associated with the Q_y absorption of P. Vibronic satellites of P due to modes in the 1300–1700-cm^{-1} region would lie in the region of the $Q_y(0,0)$ band(s) of the accessory BChls.

The question remains as to why the low-frequency modes of P, particularly those below 200 cm^{-1}, exhibit unusually large S values. The S values of these modes appear to be 5–15 times larger than is normal for BChl pigments. Typically, out-of-plane deformations are not strongly coupled to $\pi\pi^*$ transitions of tetrapyrrolic macrocycles because the electronic transition dipoles are primarily in-plane (Schick & Bocian, 1987). In nonplanar ring systems, the out-of-plane modes exhibit stronger RR scattering because the transition dipole acquires some amount of out-of-plane character (Li et al., 1989). It seems unlikely that structural perturbations alone can account for the unusually large S values observed for the out-of-plane modes of the BChls that constitute P. A more reasonable origin for the large S values for the out-of-plane modes is that these vibrations are particularly effective at modulating the charge-transfer character in the Q_y excited state of P (Lösche et al., 1987, 1988; Lockhart & Boxer, 1987, 1988; Boxer et al., 1989; McDowell et al., 1991). The significant charge-transfer character in the P* state dictates that the excited-state surface has a very different equilibrium geometry than does the ground state. Consequently, deformations that modulate the interring interactions, such as out-of-plane vibrations, would be expected to exhibit strong Franck–Condon activity. In this regard, inspection of Table I reveals that most of the RR bands observed below 200 cm^{-1} can be attributed to out-of-plane deformations that involve the MgN_4 unit. These types of deformations would be expected to modulate the electronic interaction between the constituent monomers of P. The mode at 51 cm^{-1} is of particular interest. The normal coordinate calculations indicate that deformations of the MgN_4 unit do not contribute substantially to this vibration. Instead, this mode is primarily an out-of-plane translation of pyrrole ring I. Given that these rings are overlapped in the dimer (Chang et al., 1986; Allen et al., 1986), motion along this coordinate would be expected to have a significant effect on the magnitude of the intradimer electronic interaction. Indeed, the symmetrical linear combination of this mode of the two BChls of P is essentially a monomer-derived intradimer mode of the type which has been suggested as a potential candidate for strong coupling to the electronic transition (Warshel, 1980). Finally, it should be noted that the charge-transfer character in P* should also result in an out-of-plane rotation of the transition dipole moment for the absorption. In principle, this hypothesis could be tested by measuring the direction of the transition dipole moment relative to the structure of P. The rotation of the transition dipole moment could also contribute to the vibronic activity of the out-of-plane deformations. It is important to note, however, that none of the above mechanisms for strong vibronic activity of the out-of-plane modes imply that the forms of the vibrational eigenvectors are necessarily different from those of a BChl monomer.

CONCLUSIONS

The RR studies reported here indicate that both P and the accessory BChls of RCs exhibit a full complement of vibrational modes. The low-frequency modes of P appear to exhibit unusually large RR intensities which suggests that they are strongly coupled to the P* electronic transition. The RR intensities of these modes must in some way be related to the amount of charge-transfer character in the transition; however, the detailed nature of this relationship is not clear. The large number of vibronically active low-frequency modes of P indicates that the excited state potential energy surface is displaced along a number of "soft" coordinates. It remains to be determined whether these modes are also strongly coupled to the electron-transfer process or whether their vibronic activity is simply an inherent consequence of the electronic structure of P. Ultrafast time-resolved vibrational studies are needed in order to examine the participation of specific vibrational modes in the electron-transfer process.

ACKNOWLEDGMENT

We thank Drs. R. Friesner, D. Holten, S. Boxer, and R. Mathies for constructive comments on the manuscript.

REFERENCES

Allen, J. P., Feher, G., Yeates, T. O., Rees, D. C., Deisenhofer, J., Michel, H., & Huber, R. (1986) *Proc. Natl. Acad. Sci. U.S.A. 83*, 8589–8593.

Allen, J. P., Feher, G., Yeates, T. O., Komiya, H., & Rees, D. C. (1988) *Proc. Natl. Acad. Sci. U.S.A. 85*, 8487–8491.

Becker, M., Nagarajan, V., & Parson, W. W. (1991) *J. Am. Chem. Soc. 113*, 6840–6846.

Boxer, S. G., Lockhart, D. J., & Middendorf, T. R. (1986a) *Chem. Phys. Lett. 123*, 476–482.

Boxer, S. G., Middendorf, T. R., & Lockhart, D. J. (1986b) *FEBS Lett. 200*, 237–241.

Boxer, S. G., Goldstein, R. A., Lockhart, D. J., Middendorf, R. T., & Takiff, L. (1989) *J. Phys. Chem. 93*, 8280–8294.

Budil, D., Gast, P., Schiffer, M., & Norris, J. R. (1987) *Annu. Rev. Phys. Chem. 38*, 561–583.

Chang, C.-H., Tiede, D., Tang, J., Smith, U., Norris, J., & Schiffer, M. (1986) *FEBS Lett. 205*, 82–86.

Deisenhofer, J., & Michel, H. (1989a) *Science 245*, 1463–1473.

Deisenhofer, J., & Michel, H. (1989b) *EMBO J. 8*, 2149–2169.

Deisenhofer, J., Epp, O., Miki, R., Huber, R., & Michel, H. (1985) *Nature 339*, 618–624.

Donohoe, R. J., Frank, H. A., & Bocian, D. F. (1988) *Photochem. Photobiol. 48*, 531–547.

Donohoe, R. J., Dyer, R. B., Swanson, B. I., Violette, C. A., Frank, H. A., & Bocian, D. F. (1990) *J. Am. Chem. Soc. 112*, 6716–6718.

El-Kabbani, O., Chang, C.-H., Tiede, D., Norris, J., & Schiffer, M. (1991) *Biochemistry 30*, 5361–5369.

Feher, G. (1989) *Annu. Rev. Biochem. 58*, 607–663.

Feher, G., Allen, J. P., Okamura, M. Y., & Rees, D. C. (1989) *Nature 339*, 111–116.
Friesner, R. A., & Won, Y. (1989) *Biochim. Biophys. Acta 977*, 99–122.
Funfschilling, J., & Williams, D. F. (1976) *Appl. Spectrosc. 30*, 443–446.
Hayes, J. M., & Small, G. J. (1986) *J. Phys. Chem. 90*, 4928–4931.
Hayes, J. M., Gillie, J. K., Tang, D., & Small, G. J. (1988) *Biochim. Biophys. Acta 932*, 287–305.
Johnson, C. K., & Rubinovitz, R. (1990) *Appl. Spectrosc. 44*, 1103–1106.
Johnson, C. K., & Rubinovitz, R. (1991) *Spectrochim. Acta 47A*, 1413–1421.
Johnson, S. G., Tang, D., Jankowiak, R., Hayes, J. M., Small, G. J., & Tiede, D. M. (1989) *J. Phys. Chem. 93*, 5953–5957.
Johnson, S. G., Tang, D., Jankowiak, R., Hayes, J. M., Small, G. J., & Tiede, D. M. (1990) *J. Phys. Chem. 94*, 5849–5855.
Kirmaier, C., & Holten, D. (1987) *Photosynth. Res. 13*, 225–260.
Kirmaier, C., & Holten, D. (1988) *NATA ASI Ser., Ser. A 149*, 219–228.
Klevanik, A. V., Ganago, A. O., Shkuropatov, A. Y., & Shuvalov, V. A. (1988) *FEBS Lett. 237*, 61–64.
Li, X.-Y., Czernuszewicz, R. S., Kincaid, J. R., Spiro, T. G. (1989) *J. Am. Chem. Soc. 111*, 7012–7023.
Lockhart, D. J., & Boxer, S. G. (1987) *Biochemistry 26*, 664–668.
Lockhart, D. J., & Boxer, S. G. (1988) *Proc. Natl. Acad. Sci. U.S.A. 85*, 107–111.
Lösche, M., Feher, G., & Okamura, M. Y. (1987) *Proc. Natl. Acad. Sci. U.S.A. 84*, 7537–7541.
Lösche, M., Feher, G., & Okamura, M. Y. (1988) *NATO ASI Ser., Ser. A 149*, 151–164.
Lutz, M. (1984) *Adv. Infrared Raman Spectrosc. 11*, 211–300.
Lutz, M., & Robert, B. (1988) in *Biological Applications of Raman Spectroscopy* (Spiro, T. G., Ed.) Vol. 3, pp 347–411, Wiley, New York.
Lutz, M., & Mäntele, W. (1991) in *Chlorophylls* (Scheer, H., Ed.) pp 855–902, CRC Press, Boca Raton, FL.
Mattioli, T. A., Hoffman, A., Robert, B., Schrader, B., & Lutz, M. (1991) *Biochemistry 30*, 4648–4654.
McDowell, L. M., Gaul, D., Kirmaier, C., Holten, D., & Schenck, C. C. (1991) *Biochemistry 30*, 8315–8322.
McGann, W. J., & Frank, H. A. (1985) *Biochim. Biophys. Acta 807*, 101–109.
Meech, S. R., Hoff, A. J., & Wiersma, D. A. (1985) *Chem. Phys. Lett. 121*, 287–292.
Meech, S. R., Hoff, A. J., & Wiersma, D. A. (1986) *Proc. Natl. Acad. Sci. U.S.A. 83*, 9464–9468.
Myers, A. B., & Mathies, R. A. (1987) in *Biological Applications of Raman Spectroscopy* (Spiro, T. G., Ed.) Vol. 2, pp 1–58, Wiley, New York.
Noguchi, T., Furukawa, Y., & Tasumi, M. (1991) *Spectrochim. Acta 47A*, 1431–1440.
Plato, M., Möbius, K., Michel-Byerle, M. E., Bixon, M., & Jortner, J. (1988) *J. Am. Chem. Soc. 110*, 7279–7285.
Robert, B., & Lutz, M. (1988) *Biochemistry 27*, 5108–5114.
Schick, G. A., & Bocian, D. F. (1987) *Biochim. Biophys. Acta 895*, 127–154.
Shreve, A. P., Cherepy, N. J., Franzen, S., Boxer, S. G., & Mathies, R. A. (1991) *Proc. Natl. Acad. Sci. U.S.A. 88*, 11207–11211.
Tang, D., Jankowiak, R., Gillie, J. K., Small, G. J., & Tiede, D. M. (1988) *J. Phys. Chem. 92*, 4012–4015.
Warshel, A. (1980) *Proc. Natl. Acad. Sci. U.S.A. 77*, 3105–3109.
Warshel, A., & Karplus, M. (1972) *J. Am. Chem. Soc. 94*, 5612–5625.
Warshel, A., & Levit, M. (1974) *Quantum Chemistry Program Exchange*, No. 247, Indiana University.
Warshel, A., Creighton, S., & Parson, W. W. (1988) *J. Phys. Chem. 92*, 2692–2701.
Won, Y., & Friesner, R. A. (1988a) *Biochim. Biophys. Acta 935*, 9–18.
Won, Y., & Friesner, R. A. (1988b) *J. Phys. Chem. 92*, 2214–2219.
Yeates, T. O., Komiya, H., Chirino, A., Rees, D. C., Allen, J. P., & Feher, G. (1988) *Proc. Natl. Acad. Sci. U.S.A. 85*, 7993–7997.
Zankel, K., Reed, D., & Clayton, R. (1968) *Proc. Natl. Acad. Sci. U.S.A. 61*, 1243–1249.